Fisher Space Systems, LLC

Space Track Launch System
Second Stage

Phoenix Space Glider

by
Jerry F. Fisher

1.0 Introduction

The Space Track Launch System (STLS) is a two stage launch system. The first stage is a tall tower with rotating ribbons (Fisher, J.F., 2011). The tower (figure 1) is from 100-150 km in height. At the top of the tower, there is a rotating truss which supports four ribbons (two ribbons from each end of the truss) made of high strength fiber composites. Counterweights (CW) (Fisher, J.F., 2010) are attached to the end of each ribbon.

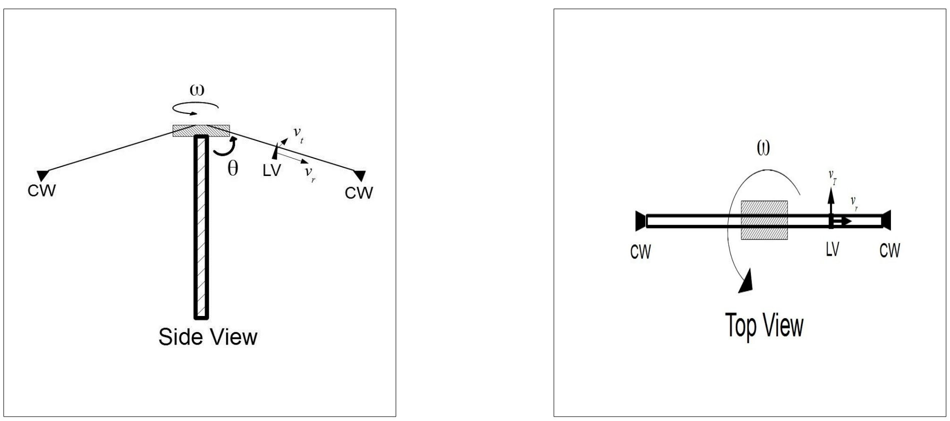

Figure 1. Space Track Launch System

The proof of concept system (Fisher, J.F., 2012) will be a 25 km tall sub-scale model of a fully operational first generation system. The proof of concept system will demonstrate the launch of a second stage suborbital launch vehicle with separation from an overcarraige on a rotating ribbon. After separation from the overcarraige, the Phoenix Space Glider (SG) will accelerate and coast to an altitude greater than 100 km, deploy and reenter using a paraglider, and land on a conventional runway (figure 2).

The Phoenix SG is a manned second stage launch vehicle designed to launch from the Space Track Launch System proof of concept tower. Two advances make the Phoenix possible. First, a standard design pressure fed hydrogen peroxide (HTP)/E85 rocket engine using mixed metal oxides (MMO) as the catalyst. With the MMO, 98% HTP can be used for the oxidizer. As shown in a previous study (Fisher, J. F., 2009), using 98% hydrogen peroxide as an oxidizer is comparable to liquid oxygen for high altitude launch. Also, HTP is room temperature storable and high density. As such, the Phoenix can be made to be low cost, simple, and reusable.

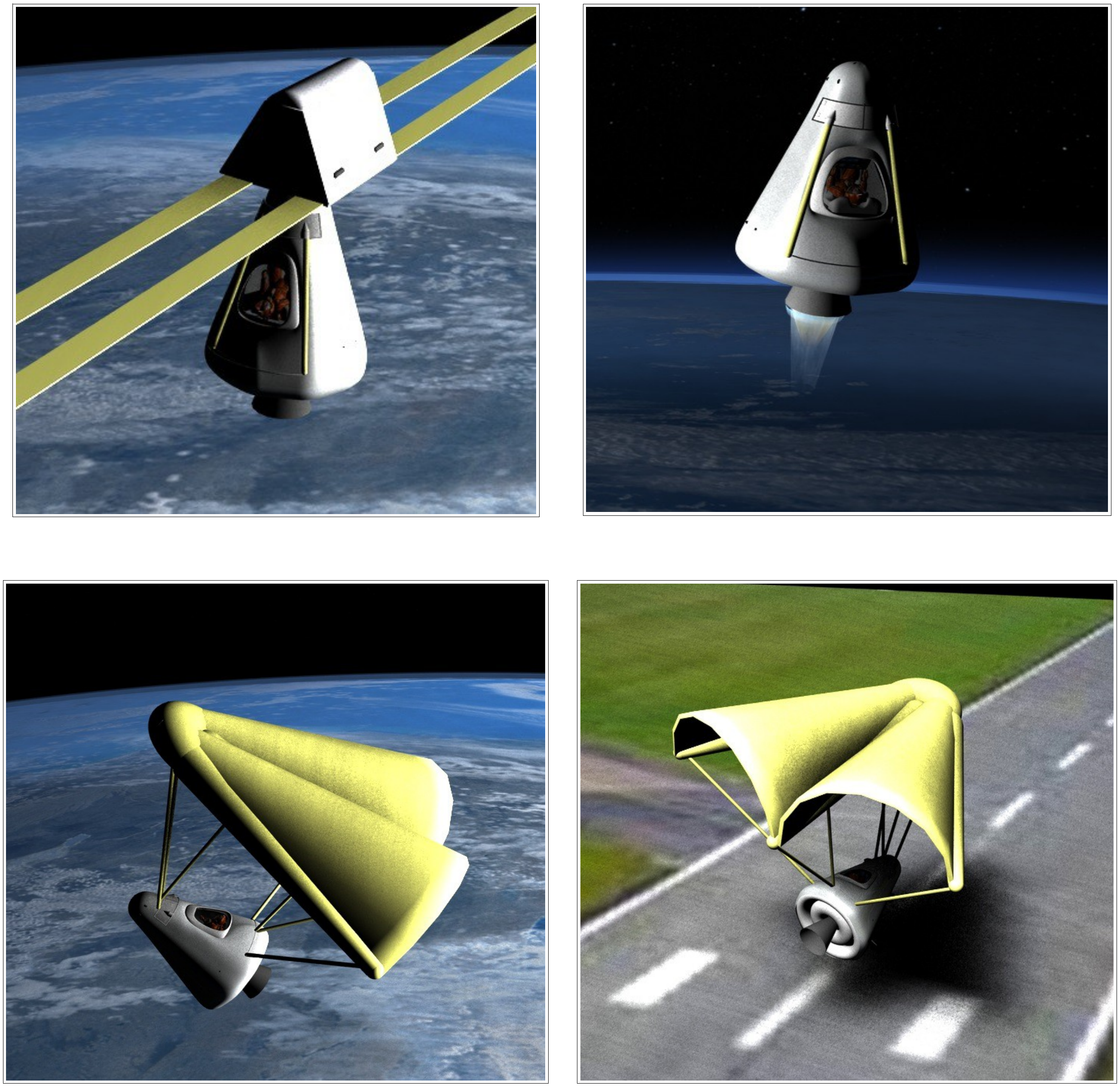

Software: Hexagon and DAZ3d
Astronaut: Mars Explorer for Genesis

Figure 2. Phoenix Launch and Recovery

The second advance is the flexible thermal protection system (FTPS) developed by NASA (Calomino, A. M., et el, 2012). The 1st generation FTPS can withstand heat fluxes of 25 W/cm^2 and the pyrogel insulator layer can absorb energies up to 5000 J/cm^2. For the Phoenix SG, an FTPS type material can be used for an inflatable keel, two inflatable booms, and the canopy for a re-entry paraglider.

Also, with HTP/E85 at combustion pressures of 100 psi, the wall temperature is approximately 1200°C with a heat flux of 24 W/cm^2. As such, the rocket engine can be made reusable by using a high melting temperature metal alloy in the combustion chamber, throat, and nozzle which is backed by an FTPS type refractory cloth and insulator. With the energy absorbing capability of the insulator, run times of about 200 seconds are possible before a cooling off period is required.

2.0 Phoenix Space Glider

The Phoenix SG is designed to launch from the STLS proof of concept tower. However, it can also be designed to launch from any 25 km free standing tower such as the Space Elevator tower recently patented by Thoth Technology Inc. (Quine, Brendan M., 2015). The gross liftoff mass for the Phoenix SG is about 7143 kg. At 25 km altitude, the Phoenix SG is above 95% of the atmosphere. As such, the vacuum specific impulse at a given throat to nozzle exhaust area will be at the most efficient. Also, at a 25 km altitude, launch delays due to weather will mainly depend on the weather at the landing site.

2.1 Phoenix Space Glider

The concept design for the Phoenix SG is shown in figure 3 below. The mass estimate for the Phoenix is derived using the mass estimating relationships compiled by Georgia Tech (Rohrschneider, R.R., 2002).

The Georgia Tech database uses a number of different relationships to estimate the mass of individual components for the flight vehicle. Georgia Tech recommends that the user select the relationship that results in the closest comparison to a known flight component. The main fuselage with crew cabin of the Phoenix SG is more closely related to a Mercury space capsule. Therefore, the relationships resulting in the correct weight for the Mercury space capsule will be used for the Phoenix.

Individual components for the Mercury space capsule were selected from the George Tech database, the weights were determined, added together, and compared to the end of reentry weight for the Mercury space capsule No. 20 (Project Mercury, 1963). The weight using the Georgia Tech database shows approximately a 2% difference from the end of reentry weight of the Mercury space capsule (Fisher, J. F., 2012). These relationships, as identified by the reference numbers, were used for the individual components of the Phoenix SG.

The main difference in design between Phoenix and Mercury is the method of launch (i.e. hanging from a overcarraige versus on top of a booster), the addition of the inflated paraglider for re-entry, the propellant tanks, the HTP/E85 rocket engine and nozzle, and the duration of flight and the recovery method.

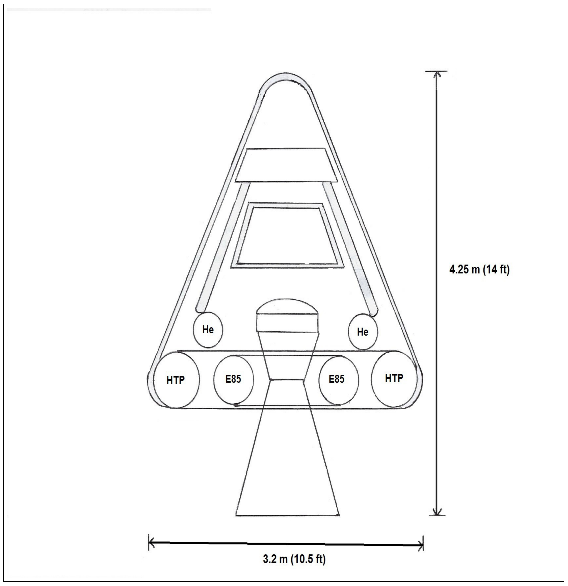

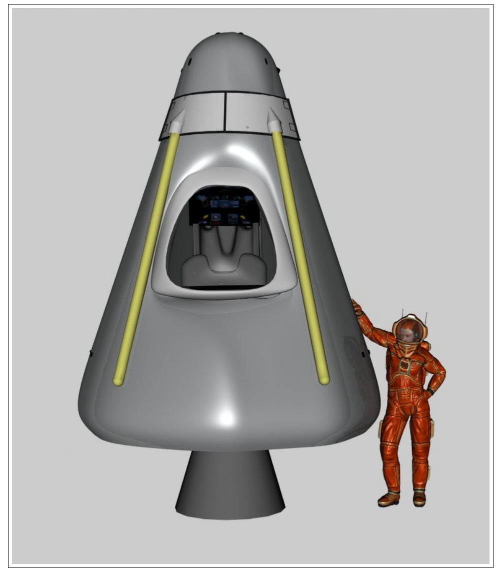

Software: Hexagon and DAZ3d
Astronaut: Mars Explorer for Genesis

Figure 3. Phoenix Space Glider

The SG will launch from the STLS proof of concept tower at an altitude of approximately 25 km, boost under thrust, coast to a peak altitude greater than 100 km, re-enter, and land on a runway using an inflated paraglider. The mass estimates are shown in table I below.

Table I. Phoenix Estimated Weight

Component	Reference	Weight Estimate (lb)
Wing Group	A2.2 Paraglider	745
Body (Fuselage & Cabin)	6	2341
Thermal Protection	6	183
Landing Gear, Pwr, & ECL	1	889
Propulsion, ECD, & SCA	3	946
Avionics & PE	4b & 7	437
Total (Sum of 1st 6 rows)	Dry Weight	5541
Dry Weight Margin	10.00%	554
Crew & Gear	4b	256
Propellants	1, 2 & 10	9397
GLOW (GLOM)		15748 (7143 kg)

2.2 Inflated Paraglider

In the 1960s, the application of the inflatable paraglider concept as a recovery device for expended booster, rockets, manned spacecraft, and instrument payloads from orbital or suborbital flight was considered by NASA and the Air Force. Both experimental and analytical investigations were conducted to evaluate the capabilities of the paraglider as such a device. The results of these studies are reported in references 9 to 16.

The paragliders of the 1960s used woven metal fabrics impregnated with high temperature silicone rubber as both an ablative coating and as an air barrier. This type of material was suitable for small re-entry spacecraft. However, as the size of the re-entry vehicle and paraglider increased, the weight of the keel and boom reached a limiting value and became impractical. Also, the race was on to reach the moon before Russia and much of the R&D funding for re-entry went to lower risk and proven technologies.

The FTPS with its refractory cloth, insulator, and air barrier have an aerial density of about 5 kg/m^2. As such, the mass of the keel, canopy, and two booms for the Phoenix SG is about 740 kg and packs in a volume of less than 0.4 m^3. The keel and two booms are about 5.3 m in length. They are tapered with the forward section 0.8 m in diameter and the rear section 0.3 m in diameter. Concept drawings of the keel, canopy, and two booms are shown in figure 4 below.

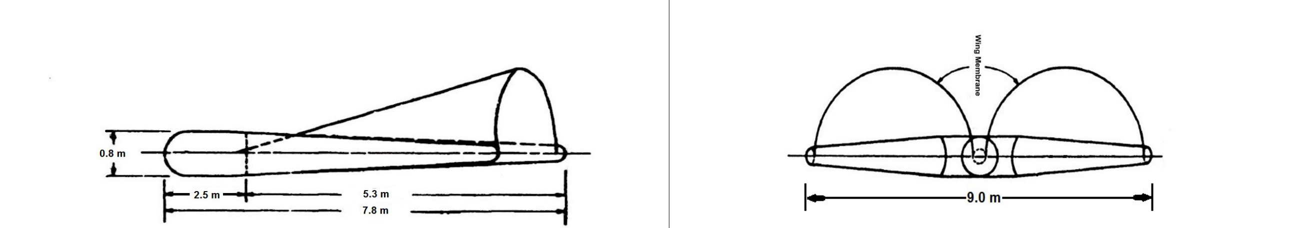

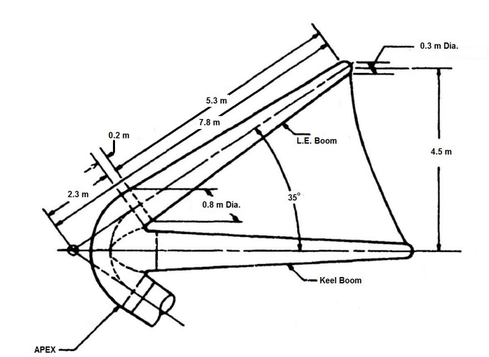

Specifications

Length	7.8 m
Wing Span	9.0 m
Sweep Angle	55 deg
Planform Area	45 m^2
Wing Loading	4900 N/m^2

Figure 4. Phoenix Space Glider

2.3 Aerodynamics

Analysis of the aerodynamic characteristics for the inflated paraglider follows a similar analysis as presented in reference 16, “Semi-Rigid or Non-Rigid Structures for Re-Entry Applications”. Analytical estimates of the pressure distribution at hypersonic speeds were made using Newtonian concepts.

The Newtonian theory assumes that the entire vertical component of stream momentum is given up to the glider. As such, the following equation results:

$$C_p = 2\sin^2(\theta) \qquad \text{(Anderson, J. D., 2006)}$$

where θ is the local flow deflection angle. The deflection angle for the canopy is given by $\alpha - \tan^{-1} dz/dx$ (Keville, J. F., 1967). Alpha is the angle of attack and dz/dx is the slope of the curve defined by the canopy in the x, z plane. The local flow deflection angles were computed by assuming that each wing membrane inflated to the shape of half of a right-circular cone, as shown in figure 5 below.

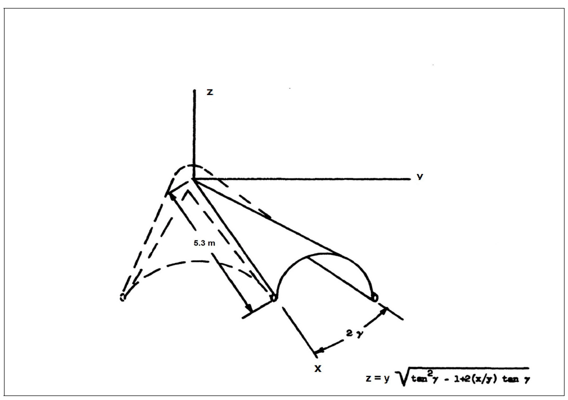

Figure 5. Space Glider Canopy

The equation for the right-circular cone as a function of x and y is given by,

$$z = y\sqrt{\tan^2\gamma - 1 + 2\left(\frac{x}{y}\right)\tan\gamma}$$

where γ is the angle of the right-circular cone. As such, dz/dx is given by,

$$\frac{dz}{dx} = \frac{\tan\gamma}{\sqrt{\tan^2\gamma - 1 + 2\left(\frac{x}{y}\right)\tan\gamma}}$$

The streamwise airfoil sections are parts of parabolas formed by cutting vertical planes parallel to the keel (i.e. planes in the x, z coordinate). The leading and trailing edges of the parabolas are described by the expressions:

$$x_{LE} = \frac{y}{\tan 2\gamma}$$

and

$$x_{TE} = l - y\tan\gamma$$

Taking the derivative, dz/dx, the pressure coefficient at any point on the panel is:

$$C_p = 2\sin^2\left(\alpha - \tan^{-1}\frac{dz}{dx}\right)$$

The pressure coefficient was integrated over the periphery of each cross-section by means of a numerical integration. At each incremental area on the parabola defined by the airfoil section, the normal and axial coefficients are calculated using the expression,

$$C_n = dA\,C_p\cos\left(\tan^{-1}\frac{dz}{dx}\right)$$

$$C_d = dA\,C_p\sin\left(\tan^{-1}\frac{dz}{dx}\right)$$

where dA is the incremental area equal to 2.3 x 10^{-6} m^2. For each angle of attack, α, the integration began by setting y=0 and calculating x_{LE}, the leading edge, and x_{TE}, the trailing edge. While the leading edge was less than the trailing edge, the normal and axial coefficients for the parabola defined by the vertical plane at y=0 was calculated. The y coordinate was advanced by 1.5 mm and the pressure distribution for the next slice of parabola was determined.

For the concept defined above, y went from 0 to 3.0 m. At the end of the run, the normal and axial coefficients had units of square meter. As such, the coefficients were divided by the canopy area defined by the half-circular cone.

Calculation of the air load distribution on the leading edge booms was made using Newtonian theory which presents the expression (Keville, J. F., 1967):

$$C_p = 2\cos^2(\theta - \alpha)\cos^2(\delta\cos(\alpha))$$

where θ is the local angle of the leading edge boom cross section relative to the x axis, and δ is the leading edge boom sweep angle measured from the y axis. A plot of the pressure distribution for α = 70° is shown in Figure 6. At a given angle of attack, the pressure distribution shown in Figure 6 is applicable to all cross sections of the boom. The pressures were numerically integrated over the periphery of each cross-section.

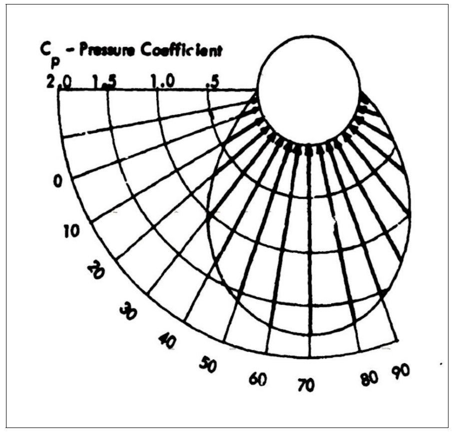

Figure 6. Pressure Distribution on Boom

With the spanwise pressure distributions established over the canopy and boom, the resulting aerodynamic coefficients and the L/D ratio during hypersonic re-entry were determined as functions of angle-of-attack and are shown in Figure 7 below.

The analysis using the Newtonian theory compares favorably with experimental values obtained at Mach 4.5 using a scale model of a flexible canopy paraglider in the hypersonic facility at the Langley Research Center (Wornom, Dewey E., and Taylor, Robert T., 1963). The variation of these coefficients with Mach number is small in the region of hypersonic re-entry velocities considered. A FORTRAN program handles the numerical integration and is included in the appendix.

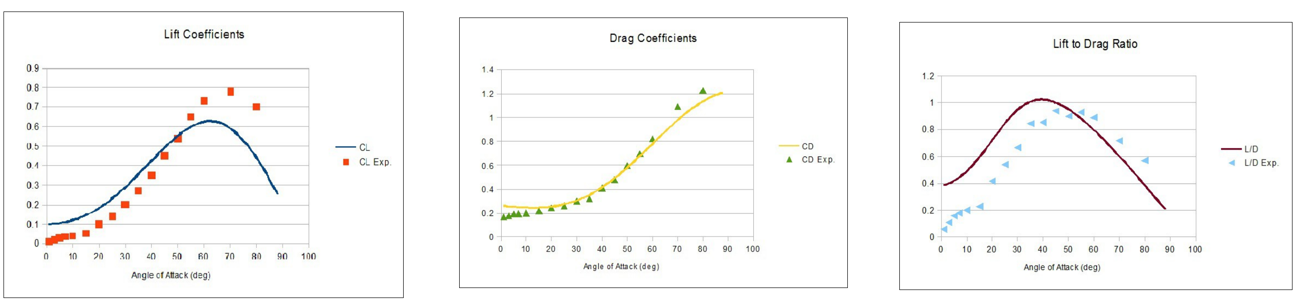

Figure 7. Aerodynamic Coefficients of Phoenix Space Glider

Consideration of a parametric study of the dynamic pressure on the boom indicated that minimum loading occurs near maximum lift coefficient. As a result, a re-entry angle of attack of 70°, which corresponds to a L/D of .6, was selected for the trajectory analysis.

2.4 Trajectory

At an angle-of-attack of 70°, the maximum heat flux and total energy absorbed are approximately 4 W/cm^2 and 120 J/cm^2 respectively. For the paraglider, the critical parameter is the dynamic pressure across the boom. It is the dynamic pressure which determines the loading and thus, the inflated pressure for the boom.

2.4.1 Boom Loading

The vertical component of the air load directly on the boom was determined from the boom air loads, the maximum dynamic pressure, and the acceleration for an angle-of-attack of 70°**.** By definition the dynamic pressure is given by,

$$q = \frac{1}{2} \rho v^{\frac{1}{2}}$$

where ρ is the freestream density and v is the freestream velocity. As shown in figure 8 below, the maximum dynamic pressure is about 2400 N/m^2. The maximum acceleration is shown in figure 9.

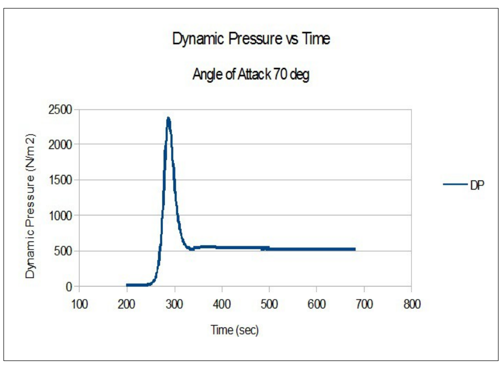

Figure 8. Dynamic Pressure

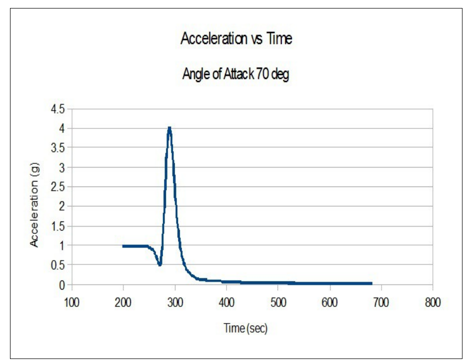

Figure 9. Acceleration

The components of boom loading due to membrane and direct air loads are shown in Figures 10 and 11. The inertial loads based on a boom weight of 160 kg and a maximum acceleration of 4.0 g's are shown in Figure 12. The combined loading used to determine the load distribution is shown in Figure 13.

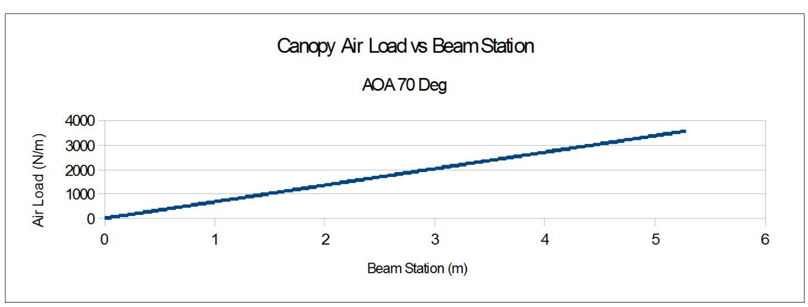

Figure 10. Canopy Air Load

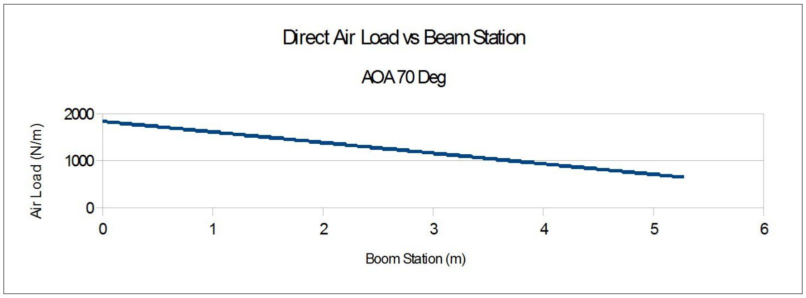

Figure 11. Direct Air Load

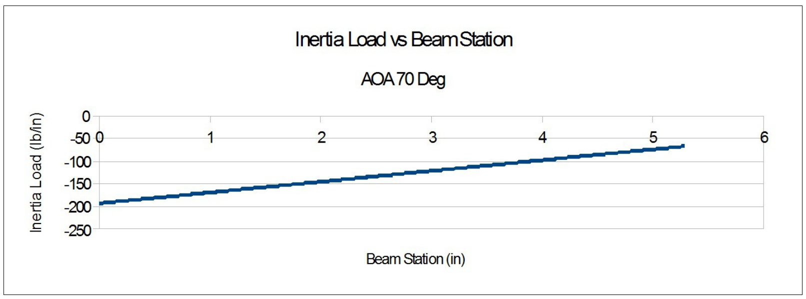

Figure 12. Inertial Load

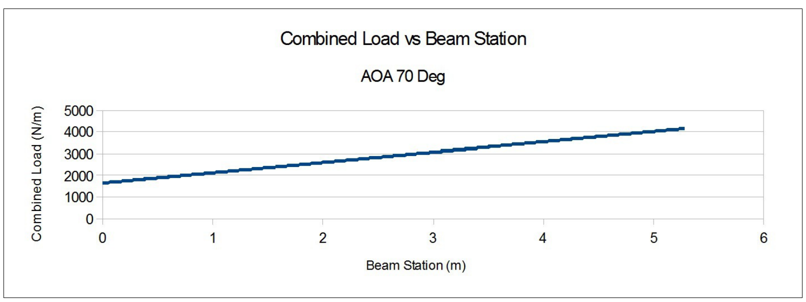

Figure 13. Combined Boom Loading

The combined boom loading was used to determine the maximum deflection at the midpoint of the boom. The boom is supported by metal wires surrounded by inflated beams connecting its front and its end. The uniform load was taken as the maximum loading equal to about 4000 N/m. The deflection was modeled by assuming simple support – uniform load which presents the equation (Shigley, J. E. and Mitchell, L. D., 1983) ,

$$y_{max} = \frac{5wl^4}{384EI}$$

where w is the load equal to 4000 N/m, l is the length of the boom equal to 5.3 m, E is the modulus of elasticity equal to 1.0 x 10^{10} N/m^2, and I is the area moment of inertia for a thin walled cylinder with an average radius of .34 m and thickness of 3.0 mm equal to 3.8 x 10^{-4} m^4. As a result, the maximum deflection at the midpoint of the boom is about 1.2 cm.

The modulus of elasticity was determined from experiments using a commercially available bi-axial weave Kevlar sleeve with a Mylar air barrier (Fisher, J. F., 2013). The results from the in house experiments agree closely with the results presented by Georgia Institute of Technology, Space System Design Lab (Hutchings, Allison L. and Braun, Robert, 2009). The test at Georgia Tech included urethane coated, silicone coated, and kapton coated Kevlar. Both the in-house test and the Georgia Tech test indicate that the Young's modulus for a Kevlar inflated beam is an order of magnitude less that that of the individual fiber. Silicone coated Kevlar was used for the Inflatable Re-Entry Vehicle Experiment (IRVE). IRVE was a test flight of a stacked toroid inflatable decelerator concept. As such, Kevlar or Vectran coated with a sealant could be a suitable material for the Phoenix SG.

2.4.2 Heat Flux and Total Energy

The stagnation point heat flux and total energy absorbed are shown in figures 14 and A15 below. The heat flux is given by (Anderson, J. D., 2006, p.349),

$$q_w = \rho^N v^M C$$

where ρ is the local freestream density, v is the freestream velocity, N = 0.5, M = 3.0, and C = 1.83 x 10^{-8} $R^{-1/2}$. This form of the heat flux is the simplest method for estimating hypersonic aerodynamic heating and is a good approximation for conceptual designs.

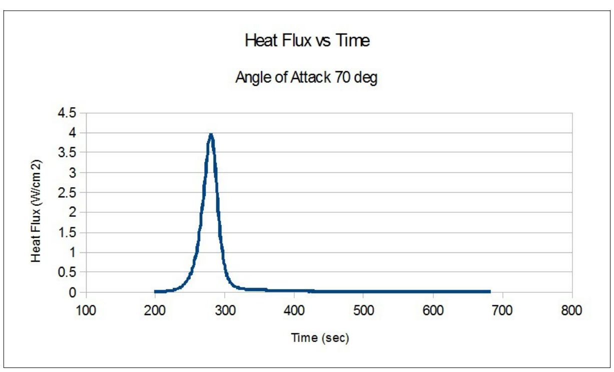

Figure 14. Stagnation Point Heat Flux

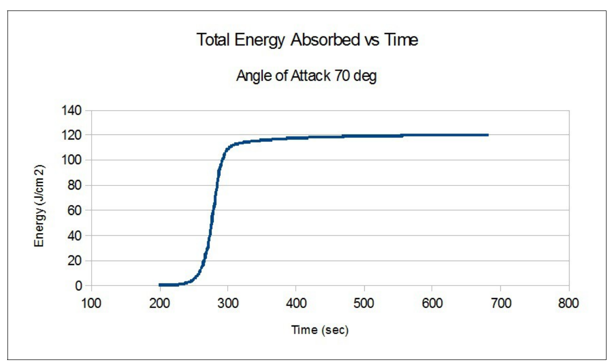

Figure 15. Total Energy Absorbed

The stagnation point heat flux is inversely proportional to the square root of the radius. In other words, the smaller the radius the greater the heat flux. Connecting the SG to the paraglider using only small diameter wires could produce heat fluxes and temperatures high enough to weaken or melt the support wires. Therefore, the support wires are enclosed by inflated beams made of the same FTPS as the booms and canopy and are about 10 cm in diameter. As such, the maximum stagnation point heat flux is about 4 W/cm^2 and the total energy absorbed is about 120 J/cm^2, well within the capability of the FTPS under investigation by NASA.

2.5 Flight Plan

The Phoenix SG is designed to launch from the STLS proof of concept tower at an altitude of 25 km. The launch point is only a few hundred meters from the tower, just enough to clear the tower before ejecting from the overcarraige. The objective is to demonstrate the full concept of the operational system; lifting the overcarraige/SG from ground level to 25 km, mounting the overcarraige/SG onto the rotating truss, launching from the ribbon, and recovery of both overcarraige and SG.

After launch, the Phoenix SG will thrust for approximately 50 seconds, coast to an altitude of over 100 km, inflate its paraglider, enter the atmosphere at an altitude of about 40 km with a velocity of 860 m/sec, and glide for about 400 seconds to a conventional runway landing. Total flight time is about 10 minutes. The flight plan is shown in figures 16 and 17 below.

Figure 16. Down Range Distance

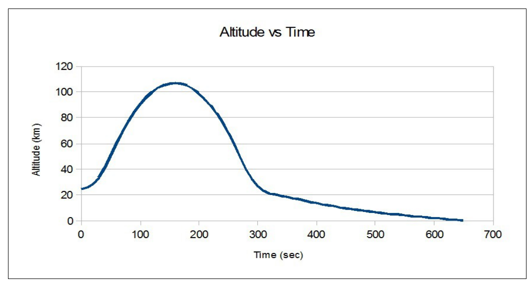

Figure 17. Flight Time

As shown in figure 16, the down range distance at landing is about 38 km. The Phoenix SG can fly to any nearby runway or return to the launch point. To return to the launch point, Phoenix can execute a 2g turn at about 15 km down range and still have enough range to make it back to the launch point. Approach speed is about 50 m/sec. Flaring would reduce the velocity to about 25 m/sec, the landing speed of a Cessna Club. Since piloting a suborbital launch vehicle requires, as a minimum, an instrument rating, the future astronaut can step out of a Cessna and into the Phoenix with minimal training.

2.6 HTP/E85 Rocket Engine

The propellant for the single rocket engine is 98% hydrogen peroxide and E85, both are readily available. The HTP passes through a mixed metal oxide catalyst consisting of cobalt, manganese, and aluminum oxides. Cobalt and manganese are transition metals which act as catalyst for the HTP. The aluminum adds structural support to the MMO. Flow control is through orifice sizing. A preliminary design of the HTP/E85 rocket engine is shown in figure A18 below. Shown in figure 19 is the rocket engine surrounded by the toroid propellant tanks.

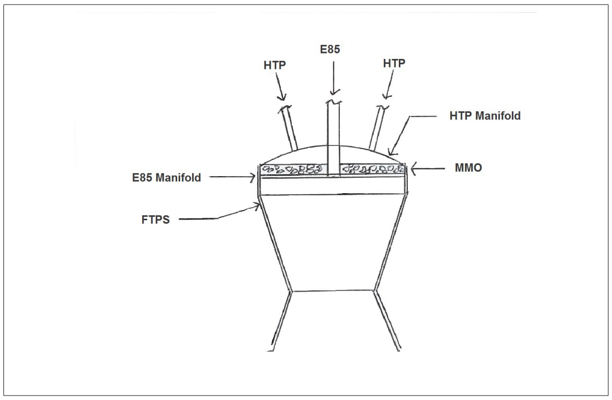

Figure 18. HTP/E85 Rocket Engine

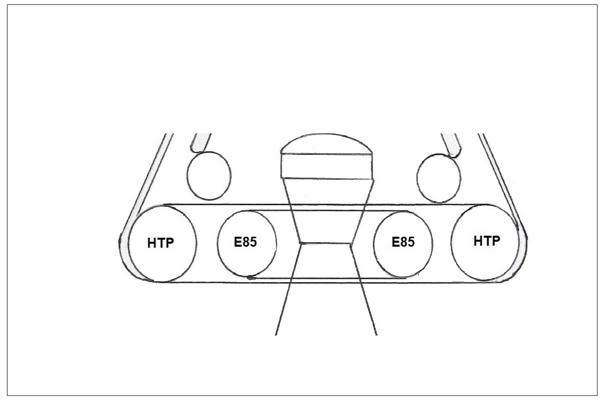

Figure 19. Propellant Tanks

There are several papers (ref. 21-24) which outline the process for developing the MMO catalyst. The process involves three different oxides each with their own phase diagrams and thermodynamic properties. It can't be done theoretically and must be done experimentally (Kovanda, F., et el, 2006). The process involves the co-precipitation of cobalt, manganese, and aluminum hydrates at the proper mole ratios while keeping the ph level constant. The slurry is then dried, crushed, peptized and calcinated in an oven. The resulting pellets have large surface area to volume ratios and can withstand temperatures over 1100°C. When used as a catalyst for HTP, the MMO pellet result in a shorter combustion chamber and smaller pressure drop across the injector as compared to silver screen catalysts.

The MMO catalyst has been used for durations of up to 5 seconds with 85% HTP. The rocket engine test was at a chamber pressure of about 50 psi and a mass flow rate of about 50 gm/s. Further research and development is required to determine if this holds for durations of 100 to 150 seconds at mass flow rates of 50 kg/s and chamber pressures of 100 psi. A crowd source funding campaign is in the works to continue the research.

The HTP/E85 rocket engine is constructed of a high melting temperature metal alloy (e.g., TZM Molybdenum) and cooled by a FTPS wrap. The FTPS surrounds the combustion chamber, throat, and nozzle. At a chamber pressure of 100 psi, the combustion temperature is about 2600 K. The wall temperature is given by,

$$h_{gc}\,(T_{aw}-T_{wg}) = \varepsilon\,\sigma\,T^4_{wg}$$

where T_{aw} is the combustion gas temperature equal to 2600 K, T_{wg} is the hot side wall temperature, ε is the emissivity equal to .95, and σ is a constant equal to 5.67 x 10^{-8} W/m^2-K^4.

The average heat transfer coefficient, h_{gc}, is a function of the Reynolds number which is itself a function of combustion gas density, velocity, and viscosity. For the combustion parameters under consideration, the average heat transfer coefficient is approximately equal to 218 W/m^2-K. As such, the hot side wall temperature is between 1100–1200°C. This results in a heat flux of 24-26 W/cm^2. The total energy absorbed for a 100 sec run time is about 2400-2600 J/cm^2, well within the capabilities of a first generation FTPS. In fact, the hot side wall temperature would be lower than presented here since the thermal conductivity of the metal alloy is not considered.

2.7 HTP/E85 Propellant Tanks

Both the 98% HTP oxidizer tank and the E85 fuel tank are lightweight composite tanks made of glass fiber with a thin walled stainless steel liner. The tanks will be toroidal in design at a pressure of 400 psi for 25+ cycles. The design is based on technologies that have been around since the 1960s (Sanger, M. J., et. El, 1966).

In a 1966 technical report, Aerojet General Corporation under contract with the Air Force, design, fabricated, and tested four, stainless-steel-lined, filament-wound tanks for the containment of nitrogen tetroxide (N_2O_4). The requirement specified storage for 30 days at an operating pressure of 350 psi and at a temperature of 110° F. The tanks were designed for a burst pressure of 761 psi with 25 cycles without failure. With the exception of burst pressure (750 vs 761 psi), all of the design requirements where met. The weight of these tanks is consistent with the mass estimating relationships compiled by Georgia Tech (Rohrschneider, R.R., 2002) with a technology reduction factor of 0.38.

3.0 Conclusion

The Phoenix suborbital launch vehicle is designed to launch from the Space Track Launch System proof of concept tower. The proof of concept system will demonstrate the launch of a second stage suborbital launch vehicle with separation from an overcarraige on a rotating ribbon. However, Phoenix can also be designed to launch from any 25 km free standing tower.

The Phoenix SG is designed to be a completely reusable manned suborbital launch vehicle consisting of a single pressure fed HTP/E85 engine with a mixed metal oxide catalyst, fiber reinforced stainless steel propellant tanks, a durable fuselage, an inflatable paraglider for controlled reentry, and a tricycle landing gear for a conventional runway landing. The mixed metal oxide catalyst and the inflatable paraglider are the only advanced concepts for the system. The remaining components will follow standard design procedures which require trial and error testing and fine tuning to achieve.

References

1. Fisher, J.F., 2011, *Space Track Launch System - Updated Oct, 2011*, www.fisherspacesystems.com /linked/stlsupdated10062011.pdf

2. Fisher, J.F., 2010, Space Track Launch System – Counterweight, www.fisherspacesystems.com /linked/stlscounterweight.pdf

3. Fisher, J.F., 2012, *Space Track Launch System - Proof of Concept System*, www.fisherspacesystems.com/linked/proof of concept tower.pdf

4. Fisher, J.F., 2009, *Space Track Launch System - Second Stage Requirements*, www.fisherspacesystems.com /linked/stls2ndstagereq.pdf

5. Calomino, A.M., Dec, J.A., Del Corso, J.A., Sullivan, R.M., Baker, E.H., Bonacuse, P.J., *Flexible Thermal Protection System Design and Margin Policy*, 9th International Planetary Probe Workshop, Toulouse, France, June 2012.

6. Quine, Brendan, M., *Space Elevator*, Patent No. US 9,085.897 B2, Thoth Technology Inc., Jul 21, 2015

7. Rohrschneider, R.R., 2002, *Development of a Mass Estimating Relationship Database for Launch Vehicle Conceptual Design*, Georgia Institute of Technology, Under the Academic Supervision of Dr. John R. Olds, AE 8900, April 26, 2002

8. Project Mercury, 1963, NASA-TM-X-51173, *Project Mercury (MODM Project)*, Quarterly Status Report ending 31 Jan 1963

9. Rogallo, Francis M., Lowry, John G., Croom, Delwin R., and Taylor, Robert T., *Preliminary Investigation of a Paraglider*, NASA TN D-443, 1960.

10. Fournier, Paul G., and Bell, B. Ann, *Low Subsonic Pressure Distributions on Three Rigid Wings Simulating Paragliders With Varied Canopy Curvature and Leading-Edge Sweep*, NASA TN D-983, 1961.

11. Taylor, Robert T., *Wind-Tunnel Investigation of Paraglider Models at Supersonic Speeds*, NASA TN D-985, 1961.

12. Hatch, Howard G. Jr., and McGowan, William A., *An Analytical Investigation of the Loads, Temperatures, and Ranges Obtained During the Recovery of Rocket Boosters by Means of a Parawing*, NASA TN D-1003, 1962.

13. Fournier, Paul G., and Bell, B. Ann, *Transonic Pressure Distributions On Three Rigid Wings Simulating Paragliders With Varied Canopy Curvature and Leading-Edge Sweep*, NASA TN D-1009, 1962.

14. Penland, Jim A., *A Study of the Aerodynamic Characteristics of a Fixed Geometry Paraglider Configuration and Three Canopies With Simulated Variable Canopy Inflation at a Mach Number of 6.6*, NASA TN D-1022, 1962.

15. Wornom, Dewey E., and Taylor, Robert T., *Aerodynamic Characteristics of a Flexible Canopy Paraglider Model at a Mach Number of 4.5 for Angles of Attack to 360º and Sideslip Angles from 0º to 90º*, NASA TN-D-1776, 1963

16. Keville, J.F., *Semi-Rigid or Non-Rigid Structures for Re-Entry Applications, Part 1: Evaluation and Design*, AFML-TR-67-310, 1967

17. Anderson, John D. Jr., *Hypersonic and High-Temperature Gas Dynamics,* Second Edition., AIAA Education

Series, 2006

18. Shigley, J. E. and Mitchell, L. D., *Mechanical Engineering Design*, Fourth Edition, McGraw-Hill Book Company, 1983

19. Fisher, J. F., 2013, *The Elastic Modulus of an Inflated Kevlar/Mylar Beam*, *ETR 20130510*, May 2013

20. Hutchings, Allison L. and Braun, Robert, *Experimental Determination of Material Properties for Inflatable Aeroshell Structures*, Georgia Institute of Technology, Space Systems Design Lab, May, 2009

21. Obalova, L., Jiratova, K., Kovanda, F., Pacultova, K., Lancy, Z., Mikulova, Z., 2005, *Catalytic decomposition of nitriuos oxide over catalysts prepared from Co/Mg – Mn/Al hydrotalcite – like compounds*, Applied Catlysis B: Environmental 60(2005), p. 289-297.

22. Kovanda, F., Grygar, T., Dornicak, V., Rojka, T., Bezdicka, P., Jiratova, K., 2004, *Thermal behaviour of Cu-Mg-Mn and Ni-Mg-Mn layered double hydroxides and characterization of formed oxides*, Applied Clay Science 28 (2005), p 121-136.

23. Grygar, T., Rojka, T., Bezdicka, P., Vecernikova, E., Kovanda, F., 2004, *Voltammetric and x-ray diffraction analysis of the early stages of the thermal crystallization of mixed Cu, Mn oxides*, J. Solid State Electochem (2004) 8, p. 252-257.

24. Kovanda, F., Rojka, T., Dobesova, J., Machovic,V., Bezdicka, P., Oblova, L., Jiratova, K, Grygar, T., 2006, *Mixed oxides obtained from Co and Mn containing layered double hydroxides; preparation, characterization, and catalytic properties*, Journal of Solid State Chemistry, 179 (2006), p. 812-823.

25. Sanger, M. J., Molho, R., and Morris, E.E., 1966, Aerojet General Corporation, *Stainless Steel Lined, Glass Filament Wound Tanks for Propellant Storage*, Technical Report AFML-TR-66-264, December 1966

APPENDIX

```
REAL AOA, GAM, DELT, DTR
!angle of attack, right circular cone angle, sweep angle, and deg to rad conv.
REAL XLE, XTE
!non-dimensional leading & trailing edge.
REAL DZDX, CP, CN, CA, CL, CD, LOD
!dzdx, pressure, normal, axial, lift, drag, & lift over drag coeffiecients.
REAL CNAREA, CAAREA, KNAREA, KAAREA, BNAREA, BAAREA, APNAREA, APAAREA, DEL
!total normal and axial coefficients, integration width.
REAL CSNAREA, CSAAREA
!Canopy planes parallel to the x, z axis.
REAL THT, Y, BLC, L
!angle subtended around boom, y-axis and boom line coordinates, length of boom.
REAL R, TEMP1, TEMP2
!radius of boom at BLC, temporary variables for boom normal and axial areas.
REAL X, Z, S, F, dA, SAC, SAB, SAA
!coordinates for radial distance, arc length on the ellispe, resultant forces.
!incremental area, surface area of canopy and boom.
REAL, PARAMETER:: PI=3.1415927
!OPEN(1,FILE='Phoenix Coefficients.txt')
!WRITE(1,*) 'AOA(deg) ','CL ','CD ','L/D '
OPEN(1,FILE='DATA.txt')
L=17.35
DTR=.0174533
AOA=1*DTR
DELT=55*DTR
GAM=17.5*DTR
SAB=54.
!Surface area of boom.
SAC=185.+.5*SAB
!Surface area of canopy.
SAA=18.
!Surface area of apex.
DO WHILE (AOA .LE. 89*DTR)
        Y=0
        CN=0
        CA=0
        CNAREA=0
        CAAREA=0
        BNAREA=0
        BAAREA=0
        DEL=.005
        DO WHILE (Y .LE. 9.95)
                XLE=Y/TAN(2*GAM)+DEL
! For some odd reason, this only works when I add the +del to initilize the loop.
                XTE=L-Y*TAN(GAM)
                DO WHILE (XLE .LE. XTE)
                        DZDX=TAN(GAM)/SQRT(TAN(GAM)**2-1+2*(XLE/Y)*TAN(GAM))
                        CP=2*(SIN(AOA-ATAN(DZDX)))**2
                        CNAREA=CNAREA+DEL**2*CP*COS(ATAN(DZDX))
                        CAAREA=CAAREA+DEL**2*CP*SIN(ATAN(DZDX))
                        XLE=XLE+DEL
                END DO
! Takes care of canopy at Y.
```

```
            IF (Y .EQ. 0) THEN
                KNAREA=CNAREA/DEL
                KNAREA=.17*(KNAREA+.1*KNAREA)
                CNAREA=CNAREA+KNAREA
                KAAREA=CAAREA/DEL
                KAAREA=.17*(KAAREA+.1*KAAREA)
                CAAREA=CAAREA+KAAREA
            END IF
! .1*KNAREA takes care of 10% greater pressure + .17 CNAREA takes care of the
! keel width.
            Y=Y+DEL
        END DO
        CNAREA=CNAREA/SAC
        CAAREA=CAAREA/SAC
        Y=0.
        BLC=0.
        DO WHILE (Y .LE. 9.95)
            THT=AOA-PI/2
            F=0.0
            S=(-.046*BLC+1.333)*DTR
            DO WHILE (THT .LE. AOA+PI/2)
                CP=2*COS(THT-AOA)**2*COS(DELT*COS(AOA))**2
                F=F+DEL*S*CP
                THT=THT+DTR
            END DO
            BNAREA=BNAREA+F*SIN(AOA)
            BAAREA=BAAREA+F*COS(AOA)
! Takes care of tapered boom.
            IF (Y .EQ. 0.) THEN
                TEMP1=BNAREA
                TEMP2=BAAREA
                BNAREA=BNAREA/DEL
                BAAREA=BAAREA/DEL
                BNAREA=.077*(BNAREA+.1*BNAREA)+TEMP1
                BAAREA=.077*(BAAREA+.1*BAAREA)+TEMP2
            END IF
! .1*BNAREA takes care of 10% greater pressure & .077 takes care of the
! apex width.

            Y=Y+DEL
            BLC=BLC+.0087
        END DO
        BNAREA=BNAREA/(SAB)
        BAAREA=BAAREA/(SAB)
        CN=CNAREA+BNAREA
        CA=CAAREA+BAAREA
        CL=CN*COS(AOA)+CA*SIN(AOA)
        CD=CN*SIN(AOA)+CA*COS(AOA)
        PRINT*,'At angle of attack =', AOA/DTR, CNAREA, CAAREA, BNAREA, BAAREA
        PRINT*, 'CL=',CL,'CD=',CD,'L/D=',CL/CD
!       WRITE(1,*) AOA/DTR, CL ,CD ,CL/CD
        WRITE(1,*) CL , CD
        AOA=AOA+DTR
END DO
END
```

